Biochimica et Biophysica Acta, 1016 (1990) 29–42
Elsevier

BBABIO 43158

Activation/inactivation and uni-site catalysis by the reconstituted ATP-synthase from chloroplasts

Petra Fromme [1] and Peter Gräber [2]

[1] *Max-Volmer-Institut für Biophysikalische und Physikalische Chemie, Technische Universität Berlin, Berlin (Germany)* and [2] *Biologisches Institut, Universität Stuttgart, Stuttgart (F.R.G.)*

(Received 31 July 1989)

Key words: Chloroplast; ATP synthase; Enzyme reconstitution; Activation; Enzyme kinetics; Uni-site catalysis

The proton-translocating ATP-synthase of chloroplasts, CF_0F_1, was isolated and reconstituted into asolectin liposomes. CF_0F_1 can exist in at least four different states, oxidized or reduced, either inactive or active. These states are characterized by different kinetics of ADP binding: There is no binding of ADP to the inactive, oxidized state, the rate constant for ADP binding to the inactive, reduced state is $7 \cdot 10^2$ $M^{-1} \cdot s^{-1}$. ADP binding to the active, reduced state occurs under deenergized conditions with 10^5 $M^{-1} \cdot s^{-1}$ and transforms the enzyme into the inactive, reduced state. Parallel to the ADP-dependent inactivation, the enzyme can also inactivate without ADP binding with a first-order rate constant of $7 \cdot 10^{-3}$ $M^{-1} \cdot s^{-1}$. With the active, reduced enzyme ATP-hydrolysis was measured under uni-site conditions as has been carried out with MF_1 (Grubmeyer, C., Cross, R.C. and Penefsky, H.S. (1982) J. Biol. Chem. 257, 12092–12100). The rate constant for ATP binding is 10^6 $M^{-1} \cdot s^{-1}$, the 'equilibrium constant' on the enzyme $EADPP_i/EATP$ is 0.4. The rate constants for P_i release and ADP release are 0.2 s^{-1} and 0.1 s^{-1}, respectively. This indicates that the enzyme carries out a complete turnover under uni-site conditions with rates much higher than that reported for MF_1.

Introduction

Membrane-bound ATP synthases of the F_0F_1-type catalyze ATP synthesis/hydrolysis coupled with a transmembrane proton transport. These ATP-synthases have a hydrophilic part, F_1, which contains the nucleotide binding sites and a hydrophobic membrane-integrated part, F_0, which is inserted into the membrane and is supposed to act as a proton channel. Although much knowledge has been accumulated during the last years about these enzymes, the mechanism of the catalyzed reaction is still unknown.

The F_1 part is able to bind a maximum of six nucleotides [1,2]. Three of the nucleotide binding sites are supposed to have catalytic properties, i.e., they can hydrolyze ATP. The function of the other nucleotide binding sites is still unknown. The nucleotide binding sites are located on the three β-subunits, presumably at the interface between α- and β-subunits (for reviews see Refs. 3, 4).

The presence of three catalytic sites raises the question whether they operate independently or in a cooperative manner. On the basis of the kinetics of oxygen exchange between water and phosphate during the catalytic reaction [5] it has been concluded that there exists a 'binding change' mechanism, i.e., the energy input by the protonation/deprotonation reactions leads to the release of ATP. Later it was proposed that the release of products from one site occurs only after binding of substrate to a second site [6]. Since there are three β-subunits (with corresponding catalytic sites) the binding change mechanism was consequently extended to include three different sites. Independent evidence for a binding change mechanism came from the result that ATP bound to one site is hydrolyzed extremely slowly, whereas binding of additional ATP to a second site accelerates ATP hydrolysis on the first site by orders of magnitude [7–9].

The cooperativity between different catalytic sites impedes the detailed investigation of the mechanism of the catalytic reaction, i.e., the coupling between proton transport and ATP synthesis. Such investigations are facilitated when only one catalytic site is occupied ('single-site conditions') and only one turnover is carried out ('single-turnover conditions'). Experimentally,

Correspondence: P. Fromme, Max-Volmer-Institut für Biophysikalische und Physikalische Chemie, Technische Universität Berlin, Strasse des 17. Juni 135, D-1000 Berlin 12, Germany.

such conditions are obtained at low concentrations, when the concentration of enzyme is higher than the concentration of substrate. A complete set of rate constants for the reaction cycle for uni-site catalysis has been obtained, allowing a complete thermodynamic and kinetic description of the reaction [10]. These results have been obtained with isolated MF_1. Measurements with submitochondrial particles indicate that similar results are obtained also for proton-transport-coupled ATP hydrolysis [11].

Similar measurements have not yet been reported for the ATP-synthase from chloroplasts. The reason for this is that CF_1 without special treatment does not hydrolyze ATP. However, CF_0F_1 can be isolated and reconstituted into asolectin liposomes. These preparations show high rates of ATP synthesis (200 s^{-1} [12] and ATP hydrolysis (20 s^{-1} [13]), i.e., the enzyme has nearly the same activity as in the thylakoid membrane. This system has the advantage that there are no other reactions interfering, as in the case of the natural membranes, and additionally ATP hydrolysis is coupled with the corresponding protolytic reactions, in contrast to the measurements with the isolated F_1.

The ATP synthase from chloroplasts exists in – at least – four different states [14]: the enzyme can be oxidized or reduced and both states either inactive or active. Under physiological conditions the enzyme is presumably in the reduced, active state [15].

In this work we describe single-site, single-turnover ATP hydrolysis catalyzed by the reconstituted, reduced, active ATP synthase from chloroplasts. Additionally, the binding of ADP to different enzyme species and the kinetics of inactivation are investigated.

Materials and Methods

Isolation and reconstitution of CF_0F_1

CF_0F_1 was isolated as described in Refs. 16–18. The CF_0F_1-containing band of the sucrose density gradient was rapidly frozen and stored under liquid nitrogen. SDS gels of these preparations are shown in Ref. 19. The isolated purified CF_0F_1 was reconstituted by detergent dialysis [20] as described in Ref. 17. Protein concentration was determined according to Ref. 21. The proteoliposomes finally contained approx. 1 μM CF_0F_1 and 30 g/l asolectin, 10 mM Na-Tricine (pH 8.0), 0.2 mM EDTA, 2.5 mM $MgCl_2$ and 0.25 mM dithiothreitol.

Determination of nucleotides

The ATP concentration was measured by the luciferin/luciferase technique (ATP-monitoring kit, LKB), using a LKB luminometer 1250: 50 μl of the luciferin/luciferase kit were added to 200 μl of buffer 1, containing 100 mM Tris-acetate (pH 7.8), 2 mM EDTA and 10 mM $MgCl_2$. Usually, the volume of the added sample was 10 μl; however, in some cases up to 100 μl were used. Each measurement was calibrated by addition of 10 μl ATP standard. Since the LKB standard contains some ADP, the standard was prepared using Na-ATP from Boehringer (No. 519981). The standard solution (10^{-4} M) was frozen in small aliquots and always diluted freshly to the appropriate concentration (between 10^{-5} M and 10^{-7} M) before use.

The ADP concentration was determined as follows: ADP was phosphorylated to ATP by addition of 5 μl phospho*enol*pyruvate (Sigma P 7127) (0.1 M in buffer 2 (buffer 1 with additionally 10 mM KCl) and 5 μl pyruvate kinase (Sigma P9136) (10 mg/ml in H_2O) to 200 μl buffer 2 and the resulting ATP concentration (i.e, the sum of ADP + ATP) was measured as described above. ADP was determined from the difference of the assays with and without pyruvate kinase and phospho*enol*pyruvate. The influence of all volume changes was taken into account.

Characterization of the proteoliposomes

Free nucleotides. 10 μl proteoliposomes were diluted with 20 μl H_2O and 10 μl of this sample were used for the determination of (ATP_{free}) and $\Sigma(ADP_{free}) + (ATP_{free})$ in two separate assays as described above.

Bound nucleotides. 10 μl proteoliposomes were denatured with 10 μl 0.6 M perchloric acid and subsequently 10 μl 1 M $KHCO_3$ was added. 10 μl of this sample were used for each luciferin/luciferase assay. The bound nucleotides were determined by the subtraction of the free nucleotides.

ATP synthesized in a $\Delta pH/\Delta\psi$ jump. 10 μl proteoliposomes were added to 50 μl of the acid solution (buffer 3) containing 30 mM sodium succinate (pH 4.9), 5 mM NaH_2PO_4, 2 mM $MgCl_2$, 0.5 mM KCl and 1 μM valinomycin, freshly added. The pH during incubation was 5.0. After 30 s of incubation, 50 μl of an alkaline solution (buffer 4) containing 200 mM Na-Tricine (pH 8.7), 120 mM KCl, 5 mM NaH_2PO_4, 2 mM $MgCl_2$ and 0.2 mM ADP were added. The final pH was 8.3. The reaction was stopped 15 s after the jump by addition of 10 μl 24% trichloroacetic acid. The concentration of ATP was measured with a 10 μl sample as described above. The ATP background was determined in the same way except that the acidic and alkaline solutions were mixed before the addition of the proteoliposomes. This background (resulting from the ATP in the ADP and from the enzyme bound ATP) was subtracted.

Nucleotides released in a $\Delta pH/\Delta\psi$ jump. The acid-base transition was carried out as described for ATP synthesis except that no ADP was present in the alkaline solution (buffer 5). 15 s after the acid-base transition, 100 μl of the reaction medium were added to the luciferin/luciferase assay and 5 s after this addition ATP and, in a separate experiment, ADP was measured as described above. The background was determined in

the same way except that the acidic and the alkaline solutions were mixed before the addition of proteoliposomes.

Reduction of CF_0F_1 in proteoliposomes

The proteoliposomes were incubated for 1.5 h with 50 mM dithiothreitol at pH 8.0 and room temperature. After the incubation the proteoliposomes can be stored on ice up to 4 h without any change in activity (ATP synthesis and nucleotide release in a $\Delta pH/\Delta\psi$ jump).

Activation of CF_0F_1 in proteoliposomes

The reduced proteoliposomes (usually 10 or 20 μl) were incubated for 15 s with a 5-fold volume of the acidic solution (buffer 3). Then the same volume of buffer 5 was added. This induces a $\Delta pH/\Delta\psi$ jump of $\Delta pH = 3.2$. The $\Delta\psi$ can be estimated to be about 60 mV [22].

Kinetics of ADP binding

ADP binding was measured after the enzyme was brought into different states: the inactive, oxidized state, E_i^{ox}, the inactive, reduced state, E_i^{red} and the active, reduced state, E_a^{red}. This was done as follows:

E_i^{ox} : The enzyme is in the inactive, oxidized state after reconstitution. The proteoliposomes (total enzyme concentration 290 nM) were incubated with 120 nM ADP in a solution containing one part buffer 3 and one part buffer 5, both without P_i. Samples were taken at different times and the concentration of free ADP was measured by luciferin/luciferase as described before.

E_i^{red} : The enzyme was reduced as described before. The measurement was done as described for E_i^{ox}.

E_a^{red} : The enzyme was reduced and then incubated for 15 s with the acidic buffer 3 in the absence of P_i. Then the same volume of buffer 5 (without P_i) was added. During this $\Delta pH/\Delta\psi$ jump about 120 nM ADP are released. The binding of ADP was measured as described for E_i^{ox}.

Separation of free nucleotides and P_i from proteoliposomes by centrifugation columns

The method of rapid separation of small molecules from proteins was described by Penefsky [23]. It can be used for the separation of small molecules from proteoliposomes with a few changes. The columns, containing Sephadex G-50 fine, were equilibrated with 1 ml buffer containing 10 mM Tricine-Na (pH 8.0), 0.2 mM EDTA, 2.5 mM $MgCl_2$ and 0.25 mM dithiothreitol. After 2 min of centrifugation at $1300 \times g$ the columns were ready for use. For the separation, 200 μl samples were layered on the column and centrifuged as described before. After centrifugation the volume of the eluate was determined. Usually, 10 to 50 μl of the solution remain on the column. However, the concentration of CF_0F_1-proteoliposomes remains constant during the centrifugation step. This was concluded from the fact that the turbidity of the solution (A_{560}) and, more significantly, the amount of ATP synthesized in a $\Delta pH/\Delta\psi$ jump is the same before and after the centrifugation.

ATP and P_i were completely separated from the liposomes as determined analytically (separating 200 μl liposome solution containing 1 mM ATP and 5 mM P_i on the column, the concentration in the eluate was smaller than 20 nM for ATP (detected by luciferin/luciferase), and smaller than 1 μM for P_i (detected by the method of Eibl and Lands [24])).

Kinetic measurements with CF_0F_1-proteoliposomes

For all experiments the enzyme was brought into the reduced, active state as described before. 15 s after activation by a $\Delta pH/\Delta\psi$ jump the reaction was started by addition of a solution containing ATP (either radioactive or unlabeled) and NH_4Cl in the same buffer as the proteoliposomes after activation. The resulting mixture is called reaction medium in the following text and contains 10 mM NH_4Cl for uncoupling. A scheme of this procedure is shown in Fig. 4. The initial nucleotide concentrations are the sum of the nucleotides released by activation and added nucleotides. The resulting ADP and ATP concentrations are determined by luciferin/luciferase for every set of experiments and are called ATP^0 and ADP^0. From this reaction mixture samples were taken at different times, t_x, and then treated differently for the following experiments:

Determination of the free concentrations of nucleotides

The free concentrations of ATP and (ATP + ADP) were determined as described for the release of nucleotides in a $\Delta pH/\Delta\psi$ jump. After the time t_x, a sample of 50 or 100 μl of the reaction medium was added to a luciferin/luciferase assay. For the measurement of (ATP + ADP) additionally pyruvate kinase and phospho*enol*pyruvate were present in the assay.

Determination of the enzyme-bound species

For these experiments the reaction medium contains either [γ-^{32}P]ATP or [^{14}C]ATP. After the reaction time t_x, the bound and free species were separated by G-50 centrifugation columns as described above. The time t_x is the start of the centrifuge. In the case of ^{32}P-labeled ATP, the samples were centrifuged into 50 μl trichloroacetic acid in order to stop the reaction after separation. After addition of 1 mM unlabeled ATP for decreasing the hydrolysis of the labeled ATP [^{32}P]P_i and [γ-^{32}P]ATP were separated as described below.

Acid quench: determination of the sum of free and enzyme-bound P_i

In these experiments the reaction medium contains [γ-^{32}P]ATP. The reaction was stopped after the reaction

time t_x by addition of trichloroacetic acid (final concentration 2% (w/v)). Then 1 mM of unlabeled ATP was added.

Cold chase

In these experiments the reaction medium contains [γ-^{32}P]ATP. After the reaction time t_x, an ATP solution containing unlabeled ATP + $MgCl_2$ (final concentration both 1 mM) in a buffer identical to the reaction medium was added. The reaction was stopped 10 s after the cold chase by addition of trichloroacetic acid (final concentration 2% (w/v)).

Separation of [^{32}P]P_i and [γ-^{32}P]ATP

The denatured samples were centrifuged 2 min at $3500 \times g$ for precipitation of the denatured proteoliposomes. 10 μl of an aqueous solution saturated with bromine were added to 150 μl of the supernatant in order to oxidize the dithiothreitol. Phosphate was extracted into isobutanol/toluene similarly as described in Ref. 25.

1 ml of a solution, containing 1% (w/w) ammonium molybdate in 0.3 M H_2SO_4 saturated with isobutanol/toluene (1 : 1) (v/v), was added to the oxidized sample. If the sample contained no P_i 10 μl 10 mM potassium phosphate buffer (pH 8.0) were added first. 200 μl of this solution (A) were counted in 4 ml scintillator Highionic fluor or 10 ml scintillator TM^{299} (both Packard), in order to detect the total radioactivity Σ[^{32}P]P_i + [γ-^{32}P]ATP. 1 ml isobutanol/toluene (1 : 1) (v/v) saturated with H_2O was added to the rest of the solution A and mixed. After phase separation, 500 μl of the organic phase were added to the same scintillators and counted, giving the amount of [^{32}P]P_i. The quench is these two types of sample does not differ significantly, so that a quench correction is not necessary. The amount of [γ-^{32}P]ATP was calculated from the difference of the two samples.

Results

For the following experiments different CF_0F_1 preparations and different reconstituted proteoliposomes have been used. The proteoliposomes have been characterized by measuring the free and bound nucleotides, the amount of nucleotides released by a $\Delta pH/\Delta\psi$ jump and the ATP yield in a $\Delta pH/\Delta\psi$ jump.

The results are summarized in Table I. The proteoliposomes contain about one bound ADP and one bound ATP. The ATP is released from the enzyme only by denaturation. About 0.25 nucleotides are released by a $\Delta pH/\Delta\psi$ jump (see also Figs. 1 and 2). The ATP yield is about 23 ATP/CF_0F_1. (the relatively small yield results from the high protein concentration in the liposomes which is necessary for measuring under single site conditions. Using lower enzyme concentrations, about

TABLE I

Characterization of proteoliposomes used in the following experiments

The data represent the average of nine reconstitutions using different enzyme preparations.

Conc. of CF_0F_1 in proteoliposomes (μM)	1.1 ±0.07
Free nucleotides	
ATP/CF_0F_1	0.01 ±0.002
ADP/CF_0F_1	0.2 ±0.06
Bound nucleotides	
ATP/CF_0F_1	1.15 ±0.05
ADP/CF_0F_1	1.06 ±0.12
Released nucleotides	
(ATP + ADP)/CF_0F_1	0.25 ±0.04
ATP/CF_0F_1	0.13 ±0.03
ATP synthesis yield ATP/CF_0F_1	23.5 ±5

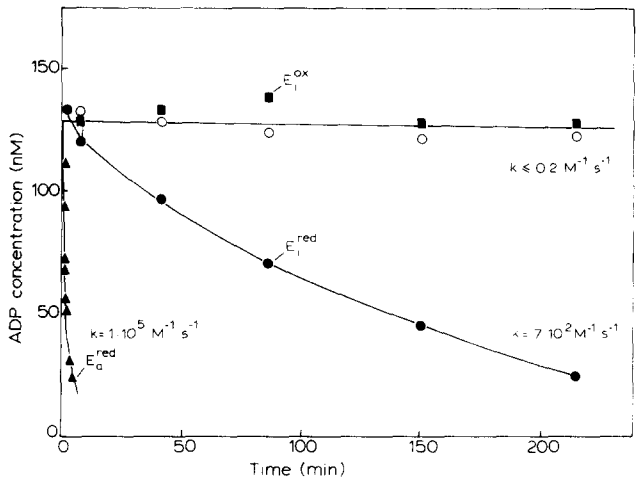

Fig. 1. Kinetics of ADP binding, when the enzyme is brought into different states as described in Materials and Methods: E_i^{ox}: The enzyme is in the inactive, oxidized state (■). E_i^{red}: The enzyme is in the inactive, reduced state (●). E_a^{red}: The enzyme is in the active, reduced state (▲). Control: proteoliposomes without enzyme (○). Rate constants are calculated from a second-order plot of the data.

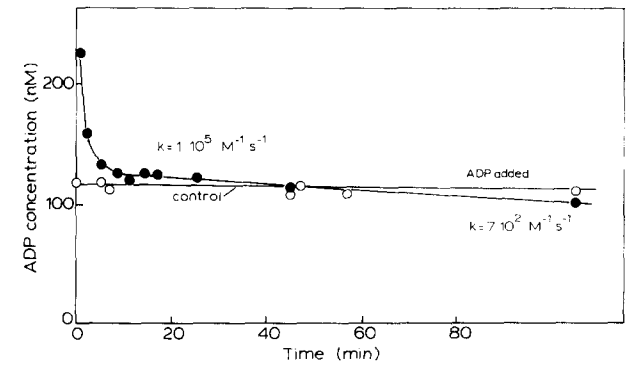

Fig. 2. Kinetics of ADP binding to the active, reduced enzyme, when, in addition to the released ADP, 115 nM ADP is added to the reaction medium. Total enzyme concentration 340 nM, active enzyme concentration 113 nM. The control shows ADP concentration without addition of enzyme.

200 ATP/CF_0F_1 are generated as reported earlier [12].)

CF_0F_1 can exist in at least four different states: an oxidized and reduced form and both forms either in an inactive or active state [13,14]. Therefore, we investigated whether these forms differ in respect to the kinetics of substrate binding and/or product release. Fig. 1 shows the kinetics of ADP binding when CF_0F_1 is brought into different states before the experiment. When the enzyme is in the inactive, oxidized state, E_i^{ox}, no ADP is bound within about 20 h. The ADP concentration used in these experiments is very low. In order to demonstrate the absence of side-reactions the ADP concentration in the reaction medium without enzyme is shown for comparison. No differences between these two experiments can be seen. A decrease of the ADP concentration of 10 nM would be easily detectable. This decrease within 20 h would correspond to a rate constant of 0.2 $M^{-1} \cdot s^{-1}$. Therefore, we must conclude that binding of ADP to the inactive, oxidized enzyme does not occur, or that at least its rate constant is no greater than 0.2 $M^{-1} \cdot s^{-1}$.

If the enzyme is brought into the inactive, reduced state, E_i^{red}, a binding of ADP is observed. Evaluation of the data results in a second-order rate constant of $7 \cdot 10^2$ $M^{-1} \cdot s^{-1}$. If the enzyme is brought into the active, reduced state, E_a^{red}, binding of ADP is much faster, and a second order plot reveals a rate constant of $1 \cdot 10^5$ $M^{-1} \cdot s^{-1}$ for the active, reduced enzyme.

When the enzyme is converted into the active state by a $\Delta pH/\Delta\psi$ jump, ADP is released, and the amount of ADP released corresponds to the amount of activated enzymes [31]. Therefore, the data for E_a^{red} in Fig. 1 show the rebinding of the ADP released during the activation step. What happens when exogeneous ADP is also added? This is shown in Fig. 2. Here 115 nM exogeneous ADP is added and about 110 nM ADP are released from the enzyme upon activation. In this case a biphasic rebinding is observed. Evaluation of the rate constants results in 10^5 $M^{-1} \cdot s^{-1}$ for the rapid phase and $7 \cdot 10^2$ $M^{-1} \cdot s^{-1}$ for the slow phase. This implies that ADP rebinding to the active form occurs with a higher rate constant until one ADP per CF_0F_1 is bound. After ADP binding, the enzyme is transformed into an inactive state, and this form binds ADP with a much lower rate constant to another nucleotide-binding site. It is also evident from the data in Fig. 2 that the latter site is not accessible when the enzyme is in the inactive, oxidized form.

In order to obtain internally consistent data, all the following experiments were carried out with the enzyme in the active, reduced state.

The binding of ADP to CF_0F_1 and the inactivation of the enzyme are strongly influenced by phosphate [26–28]. Fig. 3 shows the effect of P_i on ADP binding in a shorter time range. In the absence of phosphate (Fig. 3A), only ADP and no ATP is released into the medium

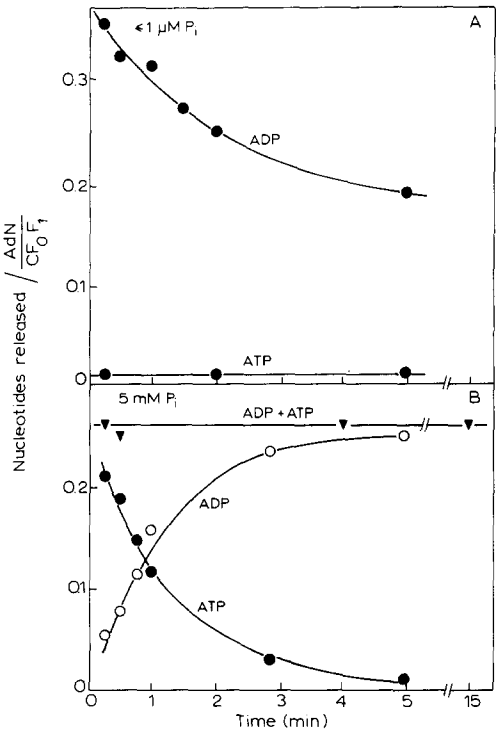

Fig. 3. Concentration of nucleotides as a function of time after activation of the enzyme by a $\Delta pH/\Delta\psi$ jump, $[CF_0F_1] = 81$ nM. (A) In the absence of P_i, $[P_i] \leq 1$ μM; (B) in the presence of 5 mM P_i.

after the $\Delta pH/\Delta\psi$ jump. Rebinding of ADP occurs again with a rate constant of 10^5 $M^{-1} \cdot s^{-1}$. Fig. 3B shows an experiment under the same conditions except that 5 mM P_i is present. In this case, at the time of the first measurement (i.e., about 15 s after the $\Delta pH/\Delta\psi$ jump), mostly ATP is found in the supernatant and this ATP is rebound to the enzyme and ADP is released concomitantly. The sum (ADP + ATP) is nearly constant during the reaction time, except for an initial phase in which 'steady-state' concentrations of the enzyme-substrate and enzyme-product complexes are built up. It has been demonstrated that after membrane energization first ADP is released and that this ADP can be subsequently phosphorylated to ATP [28,29,34]. This implies, for the experiment shown in Fig. 3B, that ADP is released after the $\Delta pH/\Delta\psi$ jump. During the time when the membrane is still energized (approx. 0.3–1 s) this ADP is rapidly rebound to the enzyme, phosphorylated and the resulting ATP is released. After the decline of the membrane energization the ATP is bound to the enzyme, hydrolyzed and ADP and P_i are released. Only the last steps are observed here.

Therefore, when ADP release in the presence of P_i is measured the sum of ADP and ATP gives the amount of active enzymes (see Table I). The ADP release in the absence of P_i is higher than in its presence. This presumably reflects that after the activation a part of the nucleotides is bound to the enzyme performing the catalytic reaction (see also Discussion).

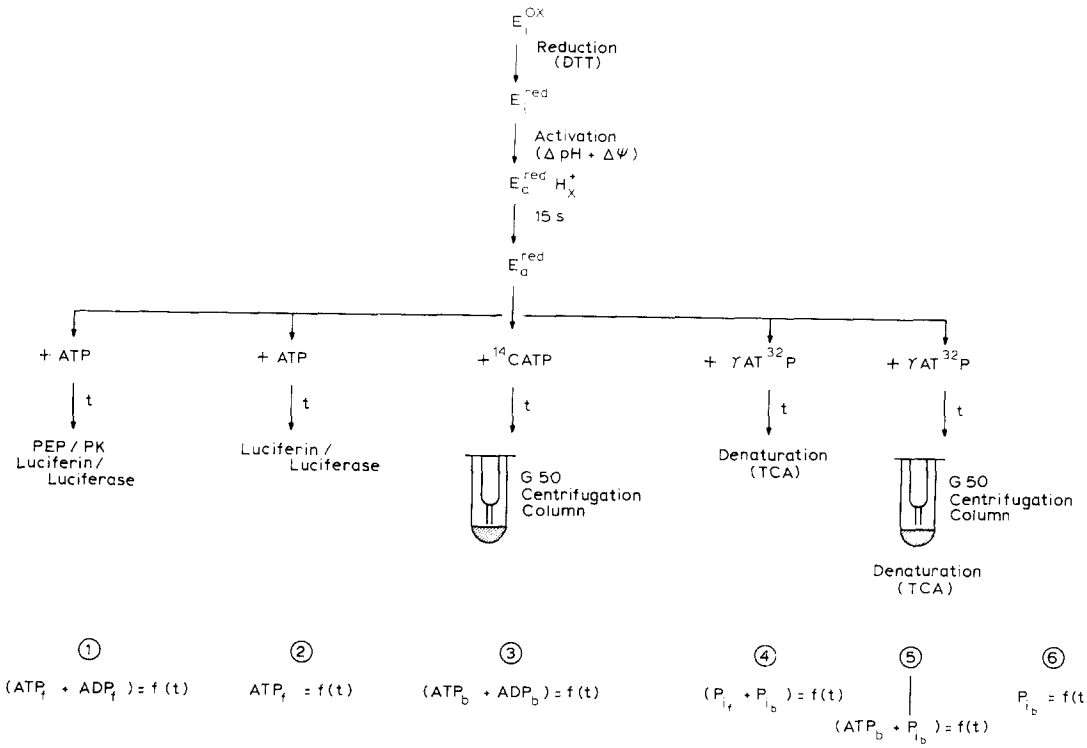

Fig. 4. Scheme of the experiment for determination of the concentrations of free and enzyme-bound ATP, ADP and P_i (for further explanations see text).

All the following experiments have been carried out with proteoliposomes when the enzyme was reduced and then activated by a $\Delta pH/\Delta\psi$ jump in the presence of 5 mM P_i.

Fig. 4 shows the experimental protocol measuring ATP hydrolysis. First the reconstituted CF_0F_1 is reduced and activated. ATP and NH_4Cl were added 15 s after activation. Typical concentrations at the beginning of the experiment are: 82 nM CF_0F_1 (about 20 nM of the enzyme is in the active form as estimated from the nucleotide release), the final ATP concentration is 22 nM, which results from 15 nM added ATP and 7 nM generated during enzyme activation.

Under these conditions, different types of experiment have been carried out as described in Materials and Methods:

(1) measurement of free (ADP + ATP);
(2) measurement of free ATP;
(3) measurement of enzyme-bound (ADP + ATP) with ^{14}C-labeled ATP using centrifugation columns for separation of free and enzyme bound nucleotides;
(4) measurement of the sum of free and enzyme-bound P_i with [γ-^{32}P]ATP;
(5) measurement of enzyme-bound (ATP + P_i) with [γ-^{32}P]ATP using centrifugation columns;
(6) measurement of enzyme-bound P_i with [γ-^{32}P]ATP using centrifugation columns.

After starting the reaction by addition of ATP, samples are taken at different times and the concentration of the different species is measured as a function of time as indicated in Fig. 4.

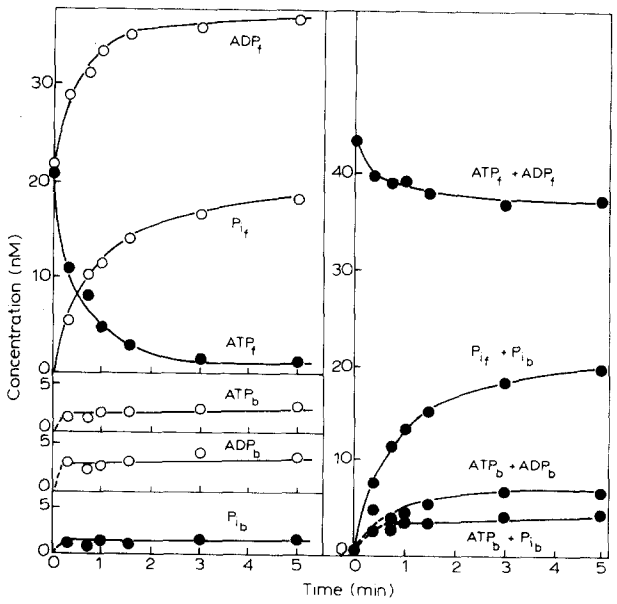

Fig. 5. Concentration of free and enzyme bound ATP, ADP and P_i as a function of the reaction time. Full circles indicate direct measurements as described in Fig. 4, open circles are determined from a combination of measurements (details, see text). f = free; b = enzyme-bound. The total enzyme concentration is 85 nM, the concentration of active enzyme is 20.2 nM.

The results are summarized in Fig. 5. The full circles indicate the direct results of the measurements (1) to (6). Open circles indicate results which are calculated from differences of measurements (1) to (6) i.e., ATP_b = (5) − (6); ADP_f = (1) − (2); P_{if} = (4) − (6) and ADP_b = (3) − (5) + (6). The indices stand for f = free and b = enzyme-bound.

A rapid decrease of free ATP is observed. The ATP bound to the enzyme is hydrolyzed to enzyme-bound ADP and enzyme-bound phosphate. Both P_i and ADP are released from the enzyme. The initial rates of P_i and ADP release are very similar and occur in the same time range as the ATP binding. Thereby, constant low levels of enzyme-bound ATP, ADP and P_i are established. The concentration of enzyme-bound P_i is about 1 nM, that of the enzyme-bound ADP is about 3 nM and the concentration of enzyme-bound ATP is about 2 nM.

It should be mentioned that, under the experimental conditions, there is no rebinding of $[^{32}P]P_i$ because the $[^{32}P]P_i$ is released into a medium containing 5 mM unlabeled P_i.

The data obtained with ^{14}C-labeled ATP show that $[^{14}C]$ADP is released. This implies, that the same adenine moiety is released as was bound to the enzyme in the previous step. This excludes that ADP from a second site (e.g., from the tightly bound ATP) is released upon binding of ATP to the first site. The data obtained with $[\gamma\text{-}^{32}P]$ATP show that also the phosphate originates from the same nucleotide which has bound to the enzyme before. According to these results the enzyme carries out a complete turnover under these conditions, regenerating the free enzyme at the end of the cycle.

At reaction times longer than 2 min the interpretation of the data becomes difficult. The level of the enzyme bound ATP, ADP and P_i remains nearly constant, although the concentration of free ATP has become so low that a decrease of the enzyme-bound species should be expected. Possibly, an inactivation of the enzyme is superimposed on the catalytic reaction.

Therefore, we measured the inactivation of the active enzyme species, E_a^{red}, as the function of time.

The enzyme was brought into the reduced, active state as described in Materials and Methods. At different times after the activating $\Delta pH/\Delta\psi$ jump the rate of ATP hydrolysis was measured. In Fig. 6 the result of such a measurement is depicted.

Fig. 6A shows the ATP concentration as a function of the reaction time when 1 μM ATP is added at different times after activation (t_x = 15 s to 5 min). From the slope of these curves the initial rate of ATP hydrolysis, $v(t_x)$, is calculated. In Fig. 6B the relative rate of ATP hydrolysis, $v(t_x)/v(t_0)$, is plotted as function of time after activation (closed circles). Since the rate of ATP-hydrolysis is proportional to the concentration of active, reduced enzymes, i.e., $v(t_x) \approx E_a^{red}$, it

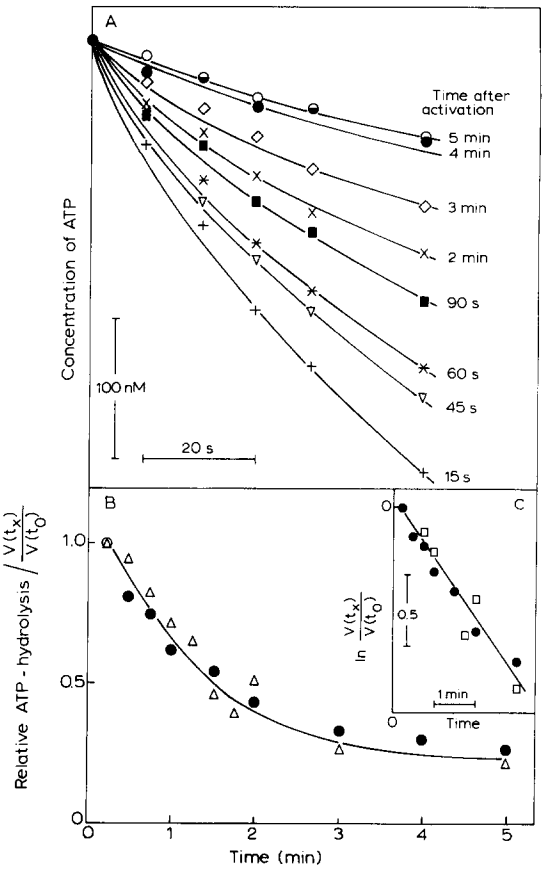

Fig. 6. Inactivation of CF_0F_1. (A) ATP hydrolysis as a function of reaction time at different times after activation by a $\Delta pH/\Delta\psi$ jump (total enzyme concentration 30 nM, active enzyme concentration 7.2 nM, $[ATP^\circ] = 1$ μM. (B) Relative rates of ATP hydrolysis as a function of time after activation measured by initial rates of ATP hydrolysis: data from (A) (circles) or from measurement of the rate of ATP-binding under 'single site' conditions (open triangles). (C) Logarithmic plot of the data from (B) indicating a first-order reaction.

results for the relative rate, if at $t_x = 0$ all enzymes are in the active, reduced state:

$$\frac{v(t_x)}{v(t_0)} = \frac{E_a^{red}}{E_a^{red}(max)}$$

This implies that the data in Fig. 6B directly show the decrease of the concentration of active enzymes.

Fig. 6C (inset) shows a logarithmic plot of these data indicating a first-order process for inactivation. The half-lifetime is 90 s giving a first-order rate constant for inactivation of $k_{in} = 7.6 \cdot 10^{-3}\ s^{-1}$.

In a second type of experiment the rate of ATP binding was measured as a function of time after activation. Under these conditions 10 nM ATP was added at different times after activation and the initial rate of ATP binding was measured. The relative initial rates of ATP binding are depicted in Fig. 6B and 6C as open triangles/squares. Both types of measurement give the same rate constants for inactivation. This implies that

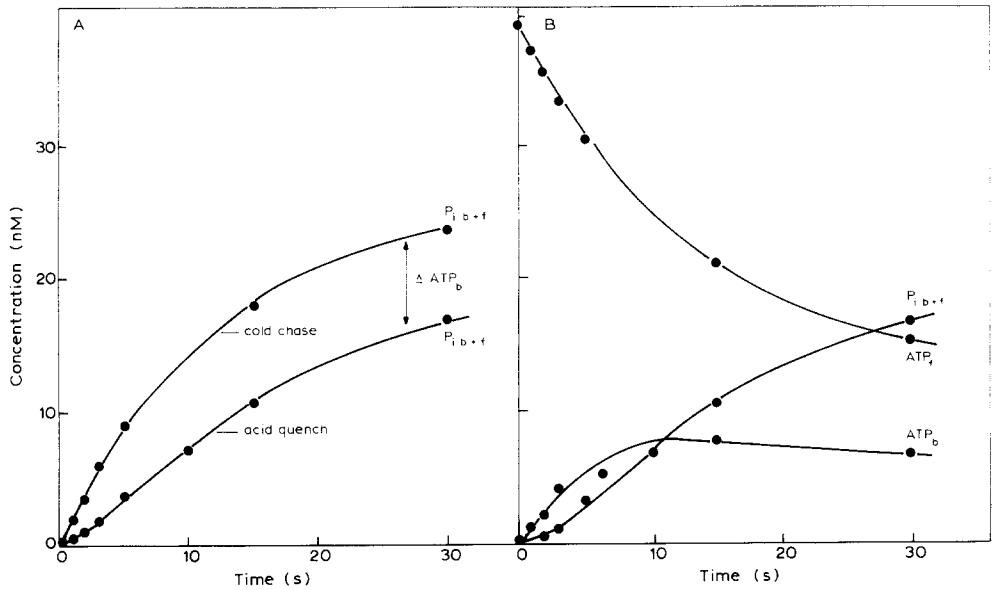

Fig. 7. Concentration of free and enzyme-bound ATP and P_i as a function of time measured by acid quench and cold chase. (A) Concentration of [^{32}P]P_i as a function of the reaction time. Total enzyme concentration 177 nM, active enzyme concentration 47.5 nM, [ATP^0] = 38.0 nM. Acid quench: the sample was denatured after the indicated reaction time. Cold chase: After the indicated reaction time 1 mM unlabelled ATP was added and 10 s later the sample was denatured. (B) Concentrations of P_i (free + bound), free ATP and enzyme-bound ATP resulting from measurement (A)(for further explanations see text). f = free; b = enzyme-bound.

already the first step of the reaction cycle (i.e., the ATP binding) is inhibited by the inactivation.

It should be mentioned that this inactivation is not coupled with a rebinding of ADP. The results, shown in Fig. 3 and 5, indicate that in the time range up to 5 min there is no significant binding of ADP in the presence of P_i. Obviously, phosphate decreases the rate of inactivation of the enzyme, due to ADP rebinding, but does not prevent the slow inactivation of the enzyme without rebinding of ADP.

According to the results shown in Fig. 6 about 10% of the active enzymes are inactivated during the first 30 s. In order to measure the kinetics of the catalytic reaction without interference by the inactivation of the enzyme, the following experiments have been carried out with higher time resolution.

The enzyme was brought into the active, reduced state and the reaction was started 15 s after the activation by addition of [γ-^{32}P]ATP and NH_4Cl as described in Materials and Methods. At different reaction times (t_x = 0–30 s) the enzyme was either denatured by addition of trichloroacetic acid (acid quench, AQ), or 1 mM unlabeled ATP was added, and 10 s later the enzyme was denatured by addition of trichloroacetic acid (cold chase, CC). In both cases, the concentration of [^{32}P]P_i was determined as a function of reaction time. The result is shown in Fig. 7A. The concentration of [^{32}P]P_i increases with reaction time and more [^{32}P]P_i is detected in the cold-chase samples.

The isotope dilution after the addition of 1 mM unlabeled ATP is so high that there is no further binding of [γ-^{32}P]ATP to the enzyme after the chase. This implies that the additional [^{32}P]P_i in the cold-chase samples must be related to hydrolysis of [γ-^{32}P]ATP, which was already bound on the enzyme before the cold chase. Parallel experiments with centrifugation columns show that there is no detectable enzyme-bound [γ-^{32}P]ATP 10 s after the chase (data not shown). Therefore, the difference between cold chase and acid quench gives the concentration of enzyme-bound ATP, i.e., $[ATP_b] = [P_i(CC)] - [P_i(AQ)]$ (see Fig. 7A).

The concentration of [^{32}P]P_i found in the acid quench represents the concentration of free and bound P_i, i.e., $[P_i(AQ)] = [P_{if}] + [P_{ib}]$. The concentration of P_i found in the cold chase in addition represents the bound ATP, i.e., $[P_i(CC)] = [P_{if}] + [P_{ib}] + [ATP_b]$.

Since all [^{32}P]P_i originates from the initial [γ-^{32}P]ATP^0, the concentration of free ATP can be calculated as follows:

$$[[\gamma\text{-}^{32}P]ATP^0] = [ATP_f] + [ATP_b] + [P_{if}] + [P_{ib}].$$

It results that:

$$[ATP_f] = [[\gamma\text{-}^{32}P]ATP^0] - [P_i(CC)].$$

Fig. 7B shows the time-course of free and enzyme-bound ATP and the sum of (free + enzyme-bound) P_i. The rate of ATP binding is the same as in Fig. 5 (rate constants see below). The concentration of enzyme-bound ATP is nearly constant between 10 s and 30 s.

From these data and additional sets of experiments, we can calculate the ratio between enzyme bound P_i and enzyme-bound ATP, i.e., the 'equilibrium

constant' * of the catalytic reaction on the enzyme. The concentration of the enzyme-bound ATP is shown already in Fig. 7B. The concentration of the enzyme-bound P_i is obtained by the following considerations [11].

At the beginning of the reaction there is no $[^{32}P]P_i$ present. When ATP is bound to the enzyme and hydrolyzed, the species $EADPP_i$ is formed first, and then ADP and P_i are released, resulting in the species EADP and EP_i as well as free ADP and P_i (see Fig. 9). As long as there is no ADP and P_i released from the enzyme, the amount of $[^{32}P]P_i$ in the acid quench experiments indicates only enzyme-bound $[^{32}P]P_i$ in the enzyme species $EADPP_i$, i.e.,

$$[P_i(AQ)] = [P_{ib}] = [EADPP_i]$$

Thus, if there is an equilibrium between EATP and $EADPP_i$, the ratio of

$$P_{ib}/[ATP_b] = \frac{[P_i(AQ)]}{[P_i(CC)] - [P_i(AQ)]}$$

should be constant, giving the equilibrium constant

$$K_2 = \frac{[EADPP_i]}{[EATP]}$$

When, in later reaction steps, ADP and P_i are released, the P_i in the acid quench experiment reflects different species:

$$[P_i(AQ)] = [EADPP_i] + [EP_i] + [P_{if}]$$

and then the ratio $[P_i(AQ)]/([P_i(CC)] - [P_i(AQ)])$ should increase.

Fig. 8 shows the result of such an evaluation. During the first 5 s the ratio of $EADPP_i/EATP$ is constant, indicating an 'equilibrium constant' $K_2 = 0.4$. After 5 s the ratio increases as expected. In the experiments with the centrifugation columns (see Fig. 5), where also P_{ib} and ATP_b was measured a ratio of 0.5 is obtained. This is practically identical with the results in Fig. 8. Since the P_{ib} in Fig. 5 reflects the sum of the enzyme species $EADPP_i$ and EP_i it must be concluded that the concentration of EP_i is low.

Discussion

Reaction scheme and calculation of rate constant

Fig. 9 shows the reaction scheme for ATP hydrolysis at one nucleotide binding site of enzyme. For the quantitative evaluation of the rate constants for the

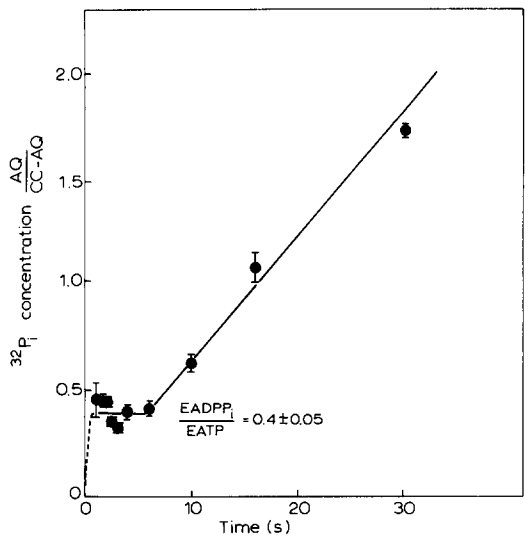

Fig. 8. Ratio of $[^{32}P]P_i$ obtained by acid quench (AQ) to enzyme-bound ATP, determined by the difference of $[^{32}P]P_i$ measured by cold chase and acid quench (CC − AQ), as a function of reaction time (details, see text).

ADP and P_i release we have to assume that the release of each of these species occurs independently of the other, i.e., $k_3 = k_6$ and $k_4 = k_5$. Also, in the reaction scheme two pathways for inactivation of the enzyme are indicated, one independent of ADP-binding, k_{in}, and one depending on ADP binding, k^*_{in}.

The rate constants have been calculated as follows. The rate constant of ATP-binding can be estimated from the initial rate of ATP binding, i.e.,

$$-\frac{d[ATP]}{dt} = k_1 \cdot [ATP] \cdot [E_a^{red}] = 1.8\ nM \cdot s^{-1}.$$

with the data from Fig. 5 it results with $[ATP^0] = 21$ nM and $[E_a^{red}] = 20.2$ nM that $k_1 = 1.2 \cdot 10^6\ M^{-1} \cdot s^{-1}$.

In the time range between 0 and 10 s, the release of the products and the inactivation of the enzyme can be neglected. A second-order plot of the data (e.g., Fig. 7)

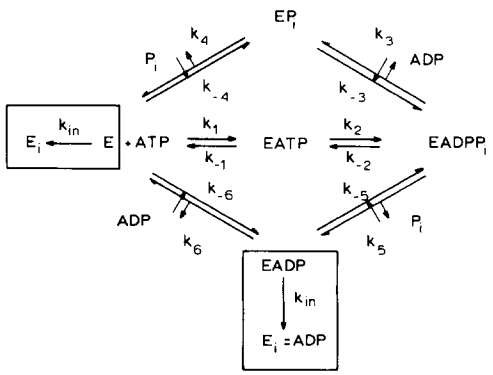

Fig. 9. Reaction scheme of ATP hydrolysis/synthesis at one nucleotide binding site. The rate constants in direction of hydrolysis have a positive sign, the rate constants in direction of ATP synthesis have a negative sign.

* In this experiment it is shown that there is a constant ratio of $EADPP_i/EATP$ during ATP hydrolysis. For determination of an equilibrium constant this value will have to be determined also in direction of ATP synthesis.

gives a straight line as expected (data not shown) with a rate constant of $k_1 = 1.1 \cdot 10^6\ M^{-1} \cdot s^{-1}$.

In the time range above 10 s free enzyme is regenerated after the reaction cycle, i.e., the concentration of free enzyme remains practically constant. In this case a pseudo-first-order reaction is expected. However, the concentration of the reduced, active enzyme is decreased by the inactivation step: $E \rightarrow E_i$. The rate constant for this step is $k_{in} = 7.6 \cdot 10^{-3}\ s^{-1}$ (Fig. 6). Therefore, the concentration of free enzyme can be calculated from:

$$E_a = E_a^0 \exp(-k_{in} t)$$

If this inactivation is taken into account, ATP binding follows pseudo-first-order kinetics, giving the same second-order rate constant. Rate constants for ATP binding have been calculated from nine measurements with different charges of proteoliposomes either by measuring the level of free ATP (as in Fig. 5) or by a combination of acid quench and cold chase experiments (as in Fig. 7). A mean value of $k_1 = (1.1 \pm 0.4) \cdot 10^6\ M^{-1} \cdot s^{-1}$ results.

The release of ADP and P_i are first-order reactions, i.e.

$$\frac{d[ADP]}{dt} = k_{3/6}[ADP_b] \quad \text{and} \quad \frac{d[P_i]}{dt} = k_{4/5}[P_{ib}]$$

The rate constants of ADP and P_i release can be calculated from the rate of ADP and P_i release at the reaction time between 10 and 30 s. In this time range the concentration of enzyme-bound species has been determined (see Fig. 5) and the inactivation of the enzyme can be neglected (see Fig. 6). The rate of ADP release is 0.24 nM s^{-1} and the rate for P_i release is 0.22 nM s^{-1}. The concentration of enzyme-bound ADP is 3.1 nM and of enzyme-bound P_i 1.2 nM. This gives the rate constants $k_{3/6} = 0.08\ s^{-1}$ for ADP release and $k_{4/5} = 0.18\ s^{-1}$ for P_i release.

The rate constant for ADP-binding was calculated from a second-order plot of the data from Figs. 1, 2 and 3, resulting in a rate constant of $k_{-3/-6} = 10^5\ M^{-1} \cdot s^{-1}$.

All these constants are collected in Table II.

TABLE II

Rate constants and equilibrium constants

Rate constant for ATP binding ($M^{-1} \cdot s^{-1}$)	k_1	$1.1 \cdot 10^6$
Rate constant for ADP binding ($M^{-1} \cdot s^{-1}$)	$k_{-3/-6}$	$1 \cdot 10^5$ [a]
Rate constant for ADP release (s^{-1})	$k_{3/6}$	0.08
Rate constant for P_i release (s^{-1})	$k_{4/5}$	0.18
Equilibrium constant	$K_2 = \frac{k_2}{k_{-2}}$	0.4
Rate constant for inactivation (s^{-1})	k_{in}	$7 \cdot 10^{-2}$

[a] Measurement in the absence of P_i (see text).

Activation and inactivation of CF_0F_1

The investigation of the catalytic mechanism of the ATP synthase from chloroplasts is impeded by the fact that the enzyme exists in four different states: oxidized or reduced and both redox states either active or inactive [14]. These different states are characterized by different rate constants for ADP binding (Fig. 1).

In this work, we investigated the reactions catalyzed by the active, reduced enzyme, E_a^{red}, since this state catalyzes reversibly ATP synthesis/hydrolysis. Presumably, this enzyme form catalyzes the proton transport coupled ATP synthesis/hydrolysis also in vivo [15,30]. Membrane energization leads to a release of tightly bound ADP from the enzyme and the enzyme becomes activated, i.e., it can now catalyze ATP synthesis (and ATP hydrolysis) [31]. Rebinding of ADP to the active enzyme leads to inactivation of ATP hydrolysis activity [26–28]. The reconstituted CF_0F_1 used in this work contains one tightly bound ATP and one tightly bound ADP. The bound ATP is released from the enzyme only by denaturation which is in accordance with earlier results [32].

Upon membrane energization about 0.25 ADP/CF_0F_1 are released. We assume that only the enzymes without the bound ADP are active enzymes. This is demonstrated by the experiment shown in Fig. 2. After activation the rebinding of ADP is biphasic: there is a fast phase, giving a second-order rate constant of $10^5\ M^{-1} \cdot s^{-1}$ and a slow phase with a rate constant of $7 \cdot 10^2\ M^{-1} \cdot s^{-1}$. The fast ADP rebinding results in an inactivation. The slow phase is attributed to a rebinding to E_i^{red}. The kinetics of rebinding changes from fast to slow when the enzyme has bound one ADP/CF_0F_1, i.e., when the amount of released ADP is rebound. This implies that the slow ADP binding to E_i^{red} occurs on a different binding site on the enzyme.

The rate constant for the ATP binding to the inactive, reduced enzyme form, E_i^{red}, is $2 \cdot 10^3\ M^{-1} \cdot s^{-1}$ [33]. This is about a factor 1000 smaller than the rate constant for ATP-binding to E_a^{red}, i.e., under our conditions, ATP binding to E_i^{red} can be neglected. The experimental observations refer to E_a^{red}, and this amount is always calculated from the nucleotide release.

The fact that only 25% of the enzymes can be activated might have different reasons:

(1) CF_0F_1 is only partially reconstituted into the liposomes. This seems to be unlikely since, after ultracentrifugation of the liposomes, no CF_1 is detected in the supernatant with antibodies.

(2) CF_0F_1 is oriented statistically in the liposomes. This would imply that only half of the enzymes can be activated.
(3) The preparation of liposomes is inhomogeneous. Electron micrographs show that small vesicles contain many CF_0F_1, whereas large vesicles contain only a few. The amount of protons in the very small vesicles is possibly too low to lead to activation of all CF_0F_1.

However, it should be mentioned that the inactive enzymes play no role in the measurements of the catalytic reaction, because they bind neither ATP nor ADP in the time range of our experiments. Upon membrane energization in the presence of phosphate, ADP is released from the enzyme first [29,31,34]. As long as the membrane is energized (about 1–2 s after the $\Delta pH/\Delta\psi$ jump with the proteoliposomes), the ADP is rebound to the enzyme, phosphorylated, and ATP is released. This can occur only if the rate constants for ADP binding and for ATP release are drastically increased under energized conditions. Finally, after denergization, the ATP is bound to the enzyme and ADP is released. These latter steps are measured at reaction times longer than 15 s (see Fig. 3B). The sum of free (ADP + ATP) remains constant after about 15 s, when constant levels of enzyme-bound ADP and ATP are established (see Figs. 5 and 7). The sum of both nucleotides is about 0.27 nM ((ATP + ADP)/CF_0F_1). In the absence of phosphate 0.34 nM (ADP/CF_0F_1) are found. The difference reflects the concentration of catalytic active enzyme-bound nucleotides, i.e., 0.07 nucleotides/CF_0F_1, which is about 20% of the active enzymes. This is in accordance with the data of Fig. 5 where 4–5 nM catalytic active bound nucleotides were found at a total active enzyme concentration of 20 nM.

According to the results shown in Fig. 5 there is an increase of the concentration of free ADP and a constant level of enzyme-bound ADP. Nevertheless, the enzyme inactivates with a half-lifetime of 90 s, as shown in Fig. 6. This implies that, in addition to the inactivation caused by ADP binding, there must be an inactivation which occurs without a previous ADP binding. We assume that there are two parallel reactions leading to inactivation: one with and one without tight binding of ADP. The second-order rate constant of ADP binding is $1 \cdot 10^5\ M^{-1} \cdot s^{-1}$. At high concentrations of ADP and enzyme (above micromolar range), the inactivation following ADP binding is the faster process. The inactivation without ADP binding can be detected only at lower concentrations of ADP. Additionally, the presence of phosphate decreases the rate of ADP dependent inactivation, so that under low ADP and high phosphate concentrations only the inactivation without ADP binding is observed (see Figs. 3 and 6).

The inactivation without ADP rebinding can be measured as an inhibition of ATP hydrolysis and as an inhibition of ATP binding (see Fig. 6). This shows that even the first step of the reaction cycle – the ATP binding to the enzyme – is inhibited. Obviously, inactivation closes the binding site for ATP on the enzyme. Therefore, in the reaction scheme (Fig. 9) we have assigned the slow inactivation to the nucleotide free enzyme, $E \rightarrow E_i$, with the rate constant k_{in}. E is also the main active enzyme species in the reaction medium (80%). However, we cannot exclude the possibility that all enzyme species are subject to this type of inactivation.

The inactivation with ADP rebinding might occur either on a catalytic or a regulatory site. Recent data of Zhou et al. [35] imply that ADP rebinding, leading to inactivation, occurs on a catalytic site. In this case, inactivation due to ADP rebinding must occur at one step of the reaction cycle shown in Fig. 9. In this scheme the inactivation due to tight binding of ADP must be related to the enzyme species EADP. However, the enzyme species EADP cannot be the inactive form per se, since ADP is released during the reaction cycle. Therefore, a second step must occur, transforming the enzyme from the active state, with ADP loosely bound, EADP, into an inactive state with a concomitant tight binding of ADP, $E_i = ADP$ with k_{in}^*.

Phosphate inhibits the inactivation due to ADP. There are two possibilities for this inhibition:
(1) Phosphate binding to a second site decreases the rate constant for ADP binding and/or the rate constant k_{in}^*.
(2) In the presence of 5 mM phosphate the enzyme species EADP is rapidly transformed into the species $EADPP_i$, so that practically no EADP is present which can be converted to $E_i = ADP$.

At present, we are unable to decide which of the two possibilities is the right one, but we prefer the latter because no additional regulatory binding site for P_i would have to be proposed.

The catalytic reaction

The data shown in Figs. 5–8 indicate that the reconstituted CF_0F_1 in its active, reduced form is able to catalyze under the experimental conditions, a complete catalytic turnover, i.e., ATP binding, hydrolysis on the enzyme, and release of products, thereby regenerating the active enzyme. From the concentration of the enzyme and substrate we expect that under these conditions only one nucleotide binding site of the enzyme is involved.

Based on the reaction scheme in Fig. 9 and the measured rate constants one can calculate the time-course of each species. This requires the simultaneous integration of all rate equations. This has been carried out by numerical integration with a personal computer using the software package LARKIN. (LARKIN is a

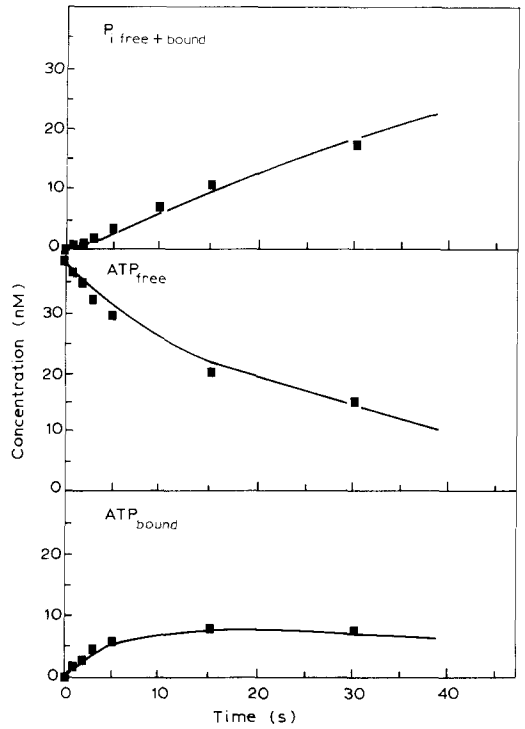

Fig. 10. Simulation of the reaction scheme of ATP hydrolysis/synthesis (see Fig. 9) for ATP hydrolysis under single site conditions with LARKIN. The results of the measurements (see Fig. 7) are depicted as full squares. The following rate constants (see Table II) are used for simulation:

rate constants

$E + ATP \rightarrow EATP$	(k_1)	$(10^6\ M^{-1}\cdot s^{-1})$
$EATP \rightleftarrows EADPP_i$	$(k_2)(k_{-2})$	$(0.48\ s^{-1})$ $(1.2\ s^{-1})$
$EADPP_i \rightarrow EADP + P_i$	(k_5)	$(0.18\ s^{-1})$
$EADP \rightleftarrows E + ADP$	$(k_6)(k_{-6})$	$(0.10\ s^{-1})(10^5\ M^{-1}\cdot s^{-1})$
$EADPP_i \rightleftarrows EP_i + ADP$	$(k_3)(k_{-3})$	$(0.10\ s^{-1})(10^5\ M^{-1}\cdot s^{-1})$
$EP_i \rightarrow E + P_i$	(k_4)	$(0.18\ s^{-1})$

The initial concentrations are (see Fig. 7): active enzyme concentration $[E^0] = 47.5$ nM, $[ATP^0] = 38$ nM and $[ADP^0] = 30$ nM; all other concentrations and rate constants are set to be zero.

program which can be used for the simulation of the kinetics of complex chemical systems [36].)

For this simulation the dissociation of ATP from the enzyme was neglected, i.e., $k_{-1} = 0$; also the rebinding of $[^{32}P]P_i$ was neglected (because of the high isotope dilution). The reaction time was limited to 30 s. In this time range the inactivation can be neglected.

Fig. 10 shows the result of such a simulation for three different species (solid lines). For comparison the measured data are depicted (data from Fig. 7). The only parameter adjusted was the rate constant, $k_2 = 0.48\ s^{-1}$. With the measured equilibrium constant $K_2 = 0.4$ this gives then $k_{-2} = 1.2\ s^{-1}$. Smaller rate constants render no good description of the experimental data. Combination of higher rate constants (with the same equilibrium constant) leads to practically the same fit as shown in Fig. 10.

We can conclude from these results that the experimental data are well described by the reaction scheme in Fig. 9 and the rate constants given in Table II.

CF_0F_1 contains three catalytic nucleotide binding sites [2,37,38]. According to the 'binding change' mechanism, ATP binding to a second site drastically increases ATP hydrolysis on the first site. Therefore, one must analyze the possibility whether actually a 'bi-site' ATP hydrolysis is observed. In order to analyze this we assumed that the release of ADP and P_i from the first site is similar to that found for MF_1 ($k_{3/6} = 10^{-4}\ s^{-1}$, $k_{4/5} = 10^{-2}\ s^{-1}$) [10] and all the other rate constants are the same as shown in Table II. For the second site we use the same rate constant for ATP binding and the same equilibrium constant as for the first site. However, all first-order rate constants in direction of ATP hydrolysis are increased, i.e. $k_2 = k_{4/5} = k_{3/6} = 100\ s^{-1}$. (These are the rate constant minima giving the measured turnover of ATP hydrolysis ($100\ s^{-1}$) [14].)

A simulation of this 'bi-site' mechanism with LARKIN shows that in this case the rate of ATP hydrolysis, i.e., the product release, is rate-limited by the binding of ATP to the second site and is too low to describe the experimental data.

Therefore, we assume that only one site is involved in ATP-hydrolysis under our experimental conditions.

Comparison with literature data

In Table III are summarized rate constants for uni-site catalysis obtained by different authors for MF_1 and CF_0F_1:

(1) The rate constants for ATP binding are of similar magnitude except for inactive CF_0F_1.
(2) The 'equilibrium constants' are similar except for inactive CF_0F_1.
(3) The rate constants for ADP binding differ significantly. ADP binding to inactive CF_0F_1 and active CF_0F_1 occurs at different sites.
(4) The rate constants for P_i release differ significantly. For MF_1 it was shown [39] that at low concentrations of Mg^{2+} the rate constant is $10^{-3}\ s^{-1}$, i.e., similar to that found in Ref. 10. In the presence of 2 mM Mg^{2+} the rate constant was increased to 0.2 s^{-1} [39,40]. This is similar to that data observed with active CF_0F_1, whereas inactive CF_0F_1 gives a rate constant of about $2 \cdot 10^{-4}\ s^{-1}$ [33].
(5) The release of ADP is the rate-limiting step of the reaction. However, the rate constants for this step differ strongly. At low concentration of Mg^{2+} a rate constant of $4 \cdot 10^{-4}$ was measured for MF_1 [10]. This is in the same range as reported for the inactive CF_0F_1 ($2 \cdot 10^{-4}\ s^{-1}$) [33]. It should be mentioned that the rate constant of ADP release in Ref. 10 could be underestimated, as was proposed in Refs. 9, 41. In the presence of 2 mM Mg^{2+} a rate constant for ADP release of $0.1\ s^{-1}$ was reported for

TABLE III

Collection of rate constants and equilibrium constants obtained for MF_1, submitochondrial particles and CF_0F_1

	MF_1 [10]	MF_1 [39]	MF_1 [39]	Submitochon. particles [11]	CF_0F_1 E_i^{ox} [33]	CF_0F_1 E_i^{red} [33]	CF_0F_1 E_a^{red}
Rate constant for ATP binding ($M^{-1}\cdot s^{-1}$)	$6.4\cdot10^6$			$5\cdot10^6$	$2\cdot10^3$	$2\cdot10^3$	$1\cdot10^6$
Rate constant for ADP binding ($M^{-1}\cdot s^{-1}$)	$1.3\cdot10^3$			$1.2\cdot10^3$	$\leqslant 0.2$	$7\cdot10^2$	$1\cdot10^5$
Rate constant for ADP release (s^{-1})	$3.6\cdot10^{-4}$		0.1	$2\cdot10^{-4}$		$2\cdot10^{-4}$	0.1
Rate constant for P_i release (s^{-1})	$2.7\cdot10^{-3}$	$1.5\cdot10^{-3}$	0.2	$2\cdot10^{-3}$	$1\cdot10^{-4}$	$2\cdot10^{-4}$	0.2
Equilibrium constant for the catalytic reaction	0.5	0.4		0.4	0.05	0.13	0.4
Reaction conditions							
Bound nucleotide ($\frac{AxP}{F_1}$)	3–5	3–5	2–3	2 ATP+ 1 ADP	1 ATP+ 1 ADP	1 ATP+ 1 ADP	1 ATP
Concentration of Mg^{2+} (mM)	0.5	0.5	2	0.5	2	2	2

MF_1 [39] similar to that for the active CF_0F_1.

(6) The combination of a lower rate constant for ATP binding and higher rate constants for ADP and P_i release leads to the effect that the concentrations of the enzyme-bound species are always very low for active, reduced CF_0F_1. Based on the total enzyme concentration the enzyme has bound only about 0.012 P_i/CF_0F_1 and 0.035 ADP/CF_0F_1. Based on the concentration of active enzymes we obtain 0.05 P_i/E_a^{red} and 0.15 ADP/E_a^{red}. This is much lower than the corresponding data for MF_1 and it drastically reduces the possibility that two ATP are bound at catalytic sites simultaneously at the same enzyme, as was proposed in Ref. 9 for MF_1.

There are several possibilities which might account for these differences:

(1) The mitochondrial enzyme is different from the enzyme of chloroplasts with regard to its kinetics.

(2) Measurements with CF_0F_1 include all protonation/deprotonation steps in the F_0 part. These partial reactions are missing in the measurements with F_1. If such differences exist they should be evident from a comparison of the data on MF_1 and submitochondrial particles. However, no differences are observed (see Table III).

(3) The enzyme can exist in different forms, active or inactive depending, for example, on phosphate or Mg^{2+} concentration. The increase of the rate constant of P_i release with Mg^{2+} concentration has been interpreted in this way [39]. However, the high rate of P_i release in a cold chase [7.8] demonstrates that the enzyme is not inactive.

(4) The enzymes contain a different number and different types of nucleotide. This might influence the catalytic reactions.

On the basis of our present knowledge it is not possible to reconcile these contradictions.

However, the results reported in this work show that CF_0F_1 is able to make a complete turnover even when only one nucleotide binding site is occupied. The kinetic properties of ATP binding and the 'equilibrium constant' are the similar for the membrane-integrated ATP synthase of chloroplasts, CF_0F_1, and the soluble part of the mitochondrial enzyme, MF_1. This indicates that:

(1) The structure of the catalytic center of these enzymes is similar and has not changed significantly during evolution; and

(2) ATP hydrolysis under the experimental conditions is not kinetically limited by proton association/dissociation. This might imply that proton pumping is not directly coupled with the catalytic reaction on the enzyme.

The rates of product release reported in this work are two or three orders of magnitude higher than those reported for MF_1 [10]. However, they are not high enough to explain the maximal turnover under substrate-saturated conditions (about 100 s^{-1}) [14]. The question whether ATP binding to a second site increases the product release from the first site is now under investigation.

Acknowledgement

This work was supported by the Deutsche Forschungsgemeinschaft, Sfb 312.

References

1 Kironde, F.A.S. and Cross, R.L. (1986) J. Biol. Chem. 261, 12544–12549.
2 Girault, G., Berger, G., Galmiche, J.-M., Andre, F. (1988) Short reports from the 5th EBEC Conference, p. 247.
3 Boyer, P.D. (1987) Biochemistry 26, 8503–8507.
4 Cross, P.L. (1988) J. Bioenerg. Biomembr. 20, 395–405.
5 Kayalar, C., Rosing, J. and Boyer, P.D. (1977) J. Biol. Chem. 252, 2486–2491.
6 Boyer, P.D. (1977) Trends Biochem. Sci. 2, 38–41.
7 Cross, R.L., Grubmeyer, C. and Penefsky, H.S. (1982) J. Biol. Chem. 257, 12101–12105.
8 Penefsky, H.S. (1988) J. Biol. Chem. 263, 6020–6022.
9 Cunningham, D. and Cross, R.C. (1988) J. Biol. Chem. 263, 18850–18856.
10 Grubmeyer, C., Cross, R.L. and Penefsky, H.S. (1982) J. Biol. Chem. 257, 12092–12100.
11 Penefsky, H.S. (1985) J. Biol. Chem. 260, 13728–13741.
12 Schmidt, G. and Gräber, P. (1987) Biochim. Biophys. Acta 890, 392–394.
13 Schmidt, G. and Gräber, P. (1987) Z. Naturforsch. 42c, 231–236.
14 Junesch, U. and Gräber, P. (1987) Biochim. Biophys. Acta 893, 275–288.
15 Mills, J.D., Mitchell, P. and Schürmann, P. (1980) FEBS Lett. 112, 173–177.
16 Pick, U. and Racker, E. (1979) J. Biol. Chem. 254, 2793–2799.
17 Schmidt, G. and Gräber, P. (1985) Biochim. Biophys. Acta 808, 46–52.
18 Fromme, P., Boekema, E.J. and Gräber, P. (1987) Z. Naturforsch. 42c, 1239–1245.
19 Fromme, P., Gräber, P. and Salnikow, J. (1987) FEBS Lett. 218, 27–30.
20 Sone, N., Yoshida, M., Hirata, H. and Kagawa, Y. (1977) J. Biochem. (Tokio) 81, 519–528.
21 Bensadoun, A. and Weinstein, D. (1976) Anal. Biochem. 70, 241–250.
22 Schmidt, G. (1987) Thesis, Technische Universität Berlin.
23 Penefsky, H.S. (1977) J. Biol. Chem. 252, 2891–2899.
24 Eibl, H. and Lands, W.E.M. (1969) Anal. Biochem. 30, 51–57.
25 Avron, M. (1960) Biochim. Biophys. Acta 40, 257–272.
26 Carmeli, C. and Lifshitz, Y. (1972) Biochim. Biophys. Acta 267, 86–95.
27 Schuman, J. and Strotmann, H. (1980) in Photosynthesis II, pp. 881–892.
28 Dunham, K.R. and Selman, B.R. (1981) J. Biol. Chem. 256, 212–218.
29 Rosing, J., Smith, D., Kayalar, C. and Boyer, P.D. (1976) Biochem. Biophys. Res. Commun. 72, 1–8.
30 Vallejos, R.H., Arana, J.L. and Rvizzini, R.A. (1983) Eur. J. Biochem. 258, 7317–7321.
31 Gräber, P., Schlodder, E. and Witt, H.T. (1977) Biochim. Biophys. Acta 461, 426–440.
32 Feierabend, B. and Schumann, J. (1988) Biochim. Biophys. Acta 932, 146–152.
33 Gräber, P., Fromme, P., Junesch, U., Schmidt, G. and Thulke, U. (1986) Ber. Bunsenges. Phys. Chem. 90, 1034–1040.
34 Strotmann, H., Bickel-Sandkötter, S. and Huchzermeyer, B. (1976) FEBS Lett. 61, 194–198.
35 Zhou, J.-M., Xue, Z., Du, Z., Melese, T. and Boyer, P.D. (1988) Biochemistry 27, 5129–5135.
36 Deuflhard, P., Bader, G. and Nowak, U. (1981) in Springer Series of Physical Chemistry 18 (Ebert, K.H., Deuflhard, P. and Jaeger, W., eds.), Springer, Berlin.
37 Xue, Z., Zhou, J.-M., Melese, T., Cross, R.L. and Boyer, P.D. (1987) Biochemistry 26, 3749–3754.
38 Xue, Z., Miller, C.G., Zhou, J.-M. and Boyer, P.D. (1987) FEBS Lett. 223, 391–394.
39 Milgrom, Y.M. and Muratiliev, M.B. (1987) FEBS Lett. 222, 32–36.
40 Milgrom, Y.M. and Muratiliev, M.B. (1987) FEBS Lett. 219, 156–160.
41 Harris, D.A. (1989) Biochim. Biophys. Acta 974, 156–162.